University of Bath

Alternative formats
If you require this document in an alternative format, please contact:
openaccess@bath.ac.uk

Mixed matrix membranes based on MIL-101 metal–organic frameworks in polymer of intrinsic microporosity PIM-1.

Muhanned Khdhayyer[1], Alexandra F. Bushell[1], Peter M. Budd[1], Martin P. Attfield*[1], Dongmei Jiang[2], Andrew D. Burrows[2], Elisa Esposito*[3], Paola Bernardo[3], Marcello Monteleone[3], Alessio Fuoco[3], Gabriele Clarizia[3], Fabio Bazzarelli[3], Amalia Gordano[3], Johannes C. Jansen[3]

[1] School of Chemistry, University of Manchester, Manchester M13 9PL, UK. E-mail: m.attfield@manchester.ac.uk

[2] Department of Chemistry, University of Bath, Claverton Down, Bath BA2 7Y, UK

[3] Institute on Membrane Technology, ITM-CNR, Via P. Bucci 17/C, 87036 Rende (CS), Italy. E-mail: e.esposito@itm.cnr.it

Abstract

This work presents a study on mixed matrix membranes (MMMs) of the polymer of intrinsic microporosity PIM-1, embedding the crystalline Cr-terephthalate metal-organic framework (MOF), known as MIL-101. Different kinds of MIL-101 were used: MIL-101 with an average particle size of ca. 0.2 µm, NanoMIL-101 (ca. 50 nm), ED-MIL-101 (MIL-101 functionalized with ethylene diamine) and NH_2-MIL-101 (MIL-101 synthesized using 2-aminoterephthalic acid instead of terephthalic acid). Permeability, diffusion and solubility coefficients and their corresponding ideal selectivities were determined for the gases He, H_2, O_2, N_2, CH_4 and CO_2 on the "as-cast" samples and after alcohol treatment. The performance of the MMMs was evaluated in relation to the Maxwell model. The addition of NH_2-MIL-101 and ED-MIL-101 does not increase the membrane performance for the CO_2/N_2 and CO_2/CH_4 separation because of an initial decrease in selectivity at low MOF content, whereas the O_2 and N_2 permeability both increase for NH_2-MIL-101. In contrast, MIL-101 and NanoMIL-101 cause a strong shift to higher permeability in the Robeson diagrams for all gas pairs, especially for CO_2, without significant change in selectivity. Unprecedented CO_2 permeabilities up to 35,600 Barrer were achieved, which are among the highest values reached with PIM-1 based mixed matrix membranes. For various gas pairs, the permeability and selectivity were far above the Robeson upper bound after alcohol treatment. Short to medium time aging shows that alcohol treated

samples with MIL-101 maintain a systematically higher permeability in time. Mixed gas permeation experiments on an aged as-cast sample with 47 vol% MIL-101 reveal that the MMM sample maintains an excellent combination of permeability and selectivity, far above the Robeson upper bound (CO_2=3,500-3,800 Barrer, CO_2/N_2= 25-27; CO_2/CH_4=21-24). This suggests good perspectives for these materials in thin film composite membranes for real applications.

Keywords: Mixed matrix membranes, PIM-1, MOFs, MIL-101, gas separation, Maxwell model

1   Introduction

Polymer membrane-based processes are recognized as low-cost and environmentally friendly alternatives to conventional gas separation processes [1]. Many polymer membranes have been investigated for gas separations, showing a trade-off between permeability and selectivity. Polymers of intrinsic microporosity (PIMs), combining a high free volume [2] with good processability, are receiving particular attention for membrane gas separation applications. The first representative of the PIM family was referred to as PIM-1 by Budd and McKeown [3,4]. PIM-1 is a spirobisindane ladder-type polymer as shown in Fig. 1A, with rigid polymer backbone and large free volume elements. Its permselectivity was used to define the 2008 Robeson upper bound, for important gas pairs such as CO_2/N_2 and CO_2/CH_4, as a consequence of its large and interconnected free volume [5–8]. These materials are prone to physical aging, which is a reduction over time of available free volume and, thus, of the permeability [9]. Even if the aging is often coupled with an improvement in the selectivity, it is not always desired because it does not allow stable operation over time [9–11]. Dimensionally more stable porous materials, such as zeolites or MOFs [12], do not have the same problem of physical aging and often combine high permeability and high selectivity. However, they are generally brittle and difficult to prepare in large areas without defects. Instead, mixed matrix membranes (MMMs) [13–17], based on inorganic or metal-organic particles dispersed in polymers, have the potential to combine synergistically the good separation performance of the fillers and the mechanical resistance of the polymers, provided that there is a good dispersion of the filler within the membrane [12,18–22]. Several nanoporous materials have been investigated for this

purpose in PIM-1, including zeolites [23] and carbon nanotubes [24], but also the non-porous graphene [25] and inorganic particles [26]. More recently, the crystalline MOFs have attracted significant attention [27–30]. These three-dimensional porous coordination polymers have versatile architectures, which combine an open porosity, large inner surface area and tuneable pore sizes and topologies [31,32]. In many cases, size selective gas transport in the MMMs is related to the pore size of MOFs, which can promote more readily the passage of small gases. While the growth of HKUST-1 and the zeolitic imidazolate framework, ZIF-8, on top of PIM-1 films lead to a reduction of the permeability [33], the dispersion of ZIF-8 in the PIM-1 matrix was found to increase the free volume, leading to higher gas permeabilities and diffusion coefficients, as well increased selectivities for gas pairs with substantial differences in kinetic diameter, such as (H_2/N_2) or (H_2/CH_4) [34]. A crucial aspect in the design of suitable MMMs is the combination of materials with a good affinity, because an interaction at the interface between the polymer matrix and the MOF particles can significantly affect the gas transport properties. Owing to the organic linkers connecting the transition metals and transition metal oxides in MOFs, a better compatibility with the continuous polymeric matrix is expected when using MOFs as fillers, rather than inorganic zeolites, in MMMs. Indeed, methods like chemical surface modification or functionalization of the MOF particles have been adopted to promote the compatibility between the fillers and the polymer matrix in order to enhance the gas separation performance of the MMM. The permeability of PIM-1 was increased from 8210 to 10,700 Barrer by the addition of functionalized UiO-66, maintaining high selectivity also in mixed gas permeation experiments [35].

The present work reports novel MMMs based on PIM-1, in which the dispersed phase consists of crystalline Cr-based MIL-101, first synthesized by Férey *et al.* [36] and indicated by Yampolskii *et al.* as a promising filler in PIM-1 [29]. MIL-101 has been dispersed in different polymers for the fabrication of MMMs for several applications. Recently, Jung *et al.* loaded MIL-101 into polystyrene-b-polybutadiene-b-polystyrene (SBS) block copolymer obtaining encouraging results for olefin/paraffin separation [37]. In pervaporation, MMMs based on modified SO_3H-MIL-101 in the hydrophilic polymer poly(vinyl alcohol) have shown large selectivities and permeabilities for water/ethylene glycol separation performance, compared with the other reported membranes [38]. In gas separation, the CO_2/CH_4 selectivity for polysulfone was enhanced by the synergic addition of MIL-101 and ZIF-8 [39].

MIL-101 (framework [Cr$_3$O(F/OH)(H$_2$O)$_2$(O$_2$CC$_6$H$_4$CO$_2$)$_3$]) has a framework structure consisting of two cages with inner free cage diameters of 2.9 nm and 3.4 nm (Fig. 1B). Entrance to these cages is through pentagonal rings of 1.2 nm diameter and hexagonal rings with 1.5 nm × 1.6 nm diameters that are large enough to admit gases and small organic molecules (Fig. 1C) [40].

The aim of this work is the demonstration that the excellent properties of PIM-1 can be further enhanced by the addition of MOFs with a very open pore structure. Different kinds of MIL-101 were dispersed in the PIM-1 matrix to study the effect of the particle size of MIL-101 and the effect of the chemical nature of amine- or ethylene diamine-functionalized MIL-101 on the MMM performance. The use of similar MOFs with different size and functionalization enabled the identification of some critical factors determining the MMM performance. Results for two batches of PIM-1 with different molar mass highlighted the importance of the continuous phase. It will be shown that a properly chosen combination of PIM-1 and MOF yields unprecedented high permeability, with a performance far above the upper bound, and this performance is maintained upon aging and for gas mixtures, yet at lower permeability and even higher selectivity.

2 Experimental

2.1 Materials

All starting materials and solvents were purchased from Sigma-Aldrich, except for 5,5',6,6'-tetrahydroxy-3,3,3',3'-tetramethyl-1,1'-spirobisindane (TTSBI, Alfa, 98%), tetrafluoroterephthalonitrile (TFTPN, Apollo Scientific Ltd., 97%), anhydrous potassium carbonate (Fisher Chemical), sodium hydroxide (Fisher Chemical) and chromium nitrate nonahydrate (Cr(NO$_3$)$_3$·9H$_2$O, Alfa, 98%). All chemicals were used as received, apart from the following chemicals: TTSBI was dissolved in methanol and re-precipitated from dichloromethane before use. TFTPN was purified by sublimation under vacuum before use. Single gases were supplied by Pirossigeno at a minimum purity of 99.9995%.

2.2 PIM-1 syntheses

Two different batches of PIM-1 (PIM-1A and PIM-1B) were synthesized from TTBSI and TFTPN by a step polymerization involving a double aromatic nucleophilic substitution with K$_2$CO$_3$ at 65 °C for PIM-1A and 160 °C for PIM-1B as described previously [5,7,41] and

detailed in the SI. PIM-1A has M_w =97,800, M_n = 31,100 g mol^{-1} and a polydispersity M_w/M_n = 31 and PIM-1B has M_w = 112,000, M_n = 48,600 g mol^{-1} and a polydispersity M_w/M_n = 2.3.

2.3 MOF syntheses

MIL-101: Two samples of MIL-101 were prepared, the first MIL-101A using a HF-based method as described previously [40,42] and the second MIL-101B using a HF-free method as reported previously [43]. The framework structure of the materials differs slightly in that some Cr atoms have terminally bound fluoride ions in the former that are replaced by hydroxide ions in the latter. Full synthesis and activation details are provided in the SI.

NanoMIL-101: NanoMIL-101 was prepared following the method of Jiang *et al.* [44] and full synthesis and activation details are provided in the SI.

ED-MIL-101: ED-MIL-101 was synthesized by functionalising MIL-101B through coordination of the amine groups of ethylene diamine to coordinatively unsaturated chromium sites following a previously reported method [45] and full synthesis and activation details are provided in the SI.

NH₂-MIL-101: NH$_2$-MIL-101 is MIL-101 synthesized using 2-aminoterephthalic acid instead of terephthalic acid. The sample was prepared using a method based upon the work of Lin *et al.* [46] and the full synthesis and activation details are provided in the SI.
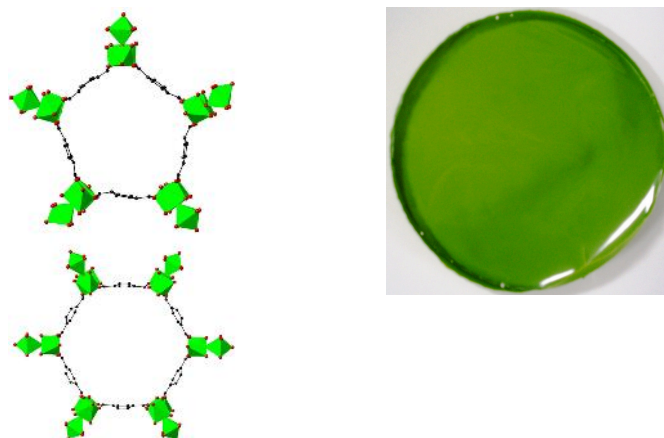
A B

C D
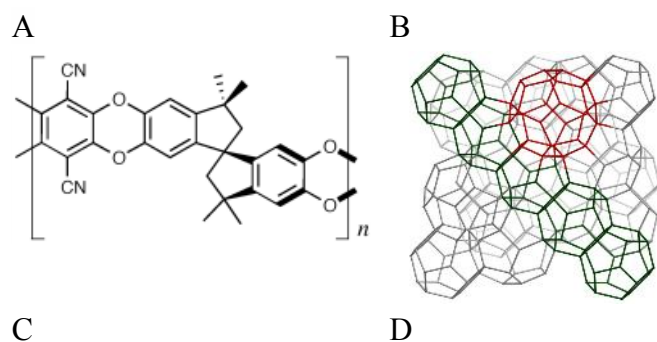
Fig. 1. (A) Repeat unit of PIM-1. (B) Porous structure of MIL-101. (C) Pentagonal and hexagonal nanometre diameter rings of MIL-101. (D) Photograph of a representative PIM-1/MIL-101 MMM.

2.4 Membrane preparation and conditioning

All the pure PIM-1 and MMMs were cast from chloroform-based solutions or suspensions that were poured into level Petri dishes and then placed in a desiccator. Slow solvent-evaporation yielded self-standing films that were green in colour for all the MMMs, as exemplified in Fig. 1D. Further details of the membrane preparations are given in the SI. The PIM-1/filler weight ratios were 10:1, 10:2, 10:3 and 10:4, corresponding to filler weight percentages of 9.1 wt%, 16.6 wt%, 23.1 wt% and 28.6 wt%, respectively. The volume fractions are calculated by SI**Error! Reference source not found.** from the polymer and filler weight fractions and their respective densities (see **Error! Reference source not found.**) and the results are given in **Error! Reference source not found.**. As-cast membranes and membranes treated with methanol (PIM-1B/MIL-101B, PIM-1B/ED-MIL-101, PIM-1B/NH$_2$-MIL-101) or ethanol (PIM-1A/MIL-101A, PIM-1A/NanoMIL-101) were tested. Alcohol treatment involved soaking the membranes for 24 h in anhydrous methanol or ethanol, followed by drying of the membrane for 24 h at 25 °C and ambient pressure. The membranes reported in this work are listed in **Error! Reference source not found.**. Membranes for aging studies were kept at ambient conditions without any control of humidity or air exposure.

2.5 Materials and membranes characterization

Materials and membranes were characterized by gel permeation chromatography (Multi Detector GPC Viscotek 2001 with two Polymer Laboratories mixed bed columns), gas sorption analysis (Micrometrics ASAP 2020 sorption analyzer), scanning electron microscopy (SEM) (Phenom Pro X desktop SEM, Phenom-World and FEI Quanta 200 ESEM) and powder X-ray diffraction (Panalytical X' Pert Pro diffractometer Model PW3040/60). Gas permeation tests of single gases were carried out at 25 °C and at a feed pressure of 1 bar, using a fixed-volume pressure increase instrument (ESSR), described elsewhere [47]. Permeability coefficients, P, and diffusion coefficients, D, were determined by the time-lag method [48]. The simplest model of permeation through dense polymeric films describes permeability as the product of a diffusion coefficient and a solubility coefficient. Thus, the apparent solubility, S, was indirectly calculated as $S = P/D$. The ideal selectivity for a pair of gases is the ratio of the permeability of the two species, $\alpha_{(A/B)} = P_A/P_B$. The values reported in the present work are effective values for the MMMs, averaged out over the polymeric and dispersed phases. Mixed gas permeation tests were carried out using a custom made constant pressure/variable volume instrument, described elsewhere [49], equipped with a quadrupole mass filter (HPR-20 QIC Benchtop residual gas analysis system, Hiden Analytical).

3 Results and discussion

3.1 Morphological characterization of MMMs

SEM images of the cross-section of the MMMs indicate that in general no significant sedimentation takes place and a good homogeneous dispersion of the MOF particles is achieved.
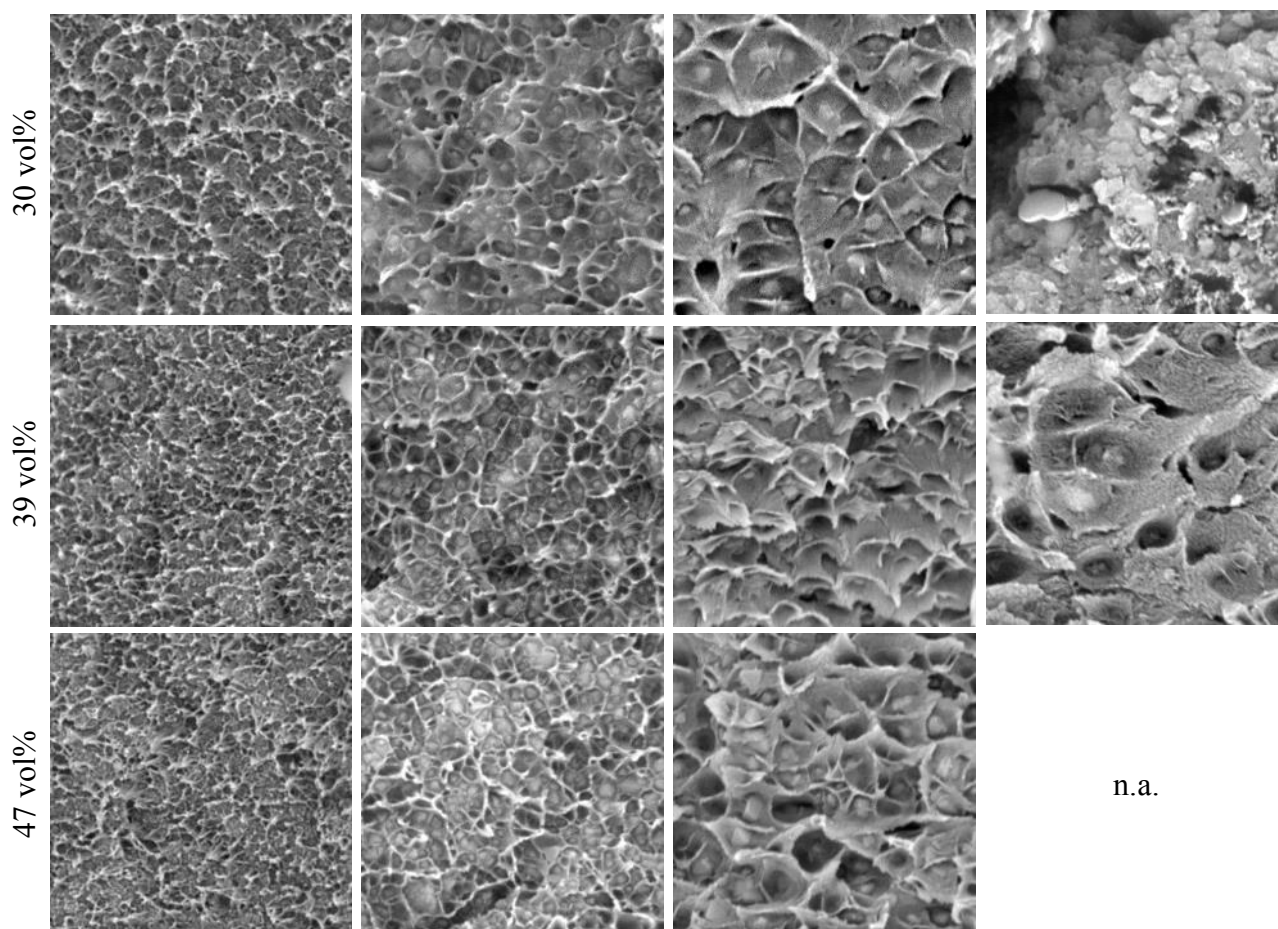
PIM-1A/NanoMIL-101   PIM-1A/MIL-101A   PIM-1B/ED-MIL-101   PIM-1B/NH$_2$-MIL-101
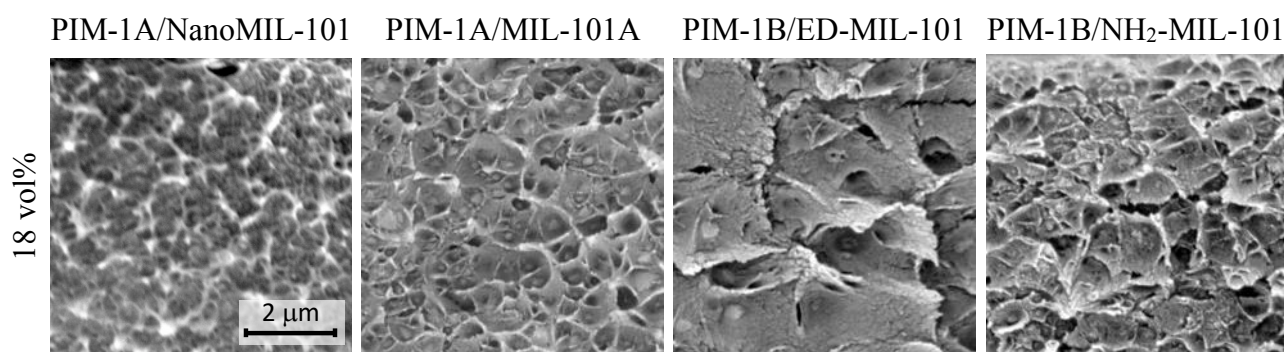
Fig. 2: SEM images of the MMMs of PIM-1A/NanoMIL-101, PIM-1A/MIL-101A, PIM-1B/ED-MIL-101 and PIM-1B/NH$_2$-MIL-101 with different MOF loadings at a magnification of 40,000 x and an accelerating voltage of 10 kV. The indicated scale bar is identical for all membranes.

Even when the MOF concentration increased from 18 vol% to the highest 47 vol%, the samples showed no significant agglomeration (Fig. 2 and **Error! Reference source not found.** and **Error! Reference source not found.**). Moreover, the SEM images do not show evidence of macro-defects, indicating a good interaction between the fillers and the polymer matrix. The polymer completely surrounds the MOF particles with circular cavities observed in the MMMs. In a few cases the MIL-101 particles seem to be embedded in an open void, but from the deformation of the polymer around these voids, it may be deduced that they are formed as a result of the tensile forces during sample fracture.

3.2 Pure gas transport properties

3.2.1 Comparison of different MOFs

Single gas permeation data were measured on the MMMs at 25 °C in the order He, H_2, O_2, N_2, CH_4 and CO_2. All permeability, diffusivity and (indirectly calculated) solubility data are given in the supporting information (**Error! Reference source not found.** - **Error! Reference source not found.**). Permeation tests were carried out on the as prepared MMMs and after alcohol treatment, which is known to open up the polymer structure and to remove residual solvent, resulting in a drastic increase of permeability [7] with similar effects for methanol and ethanol [34]. Alcohol is expected to remove also the residual solvent from MIL-101, which has sufficiently large windows and internal cavities to allow easy access of the alcohol. The permeability indeed increases upon alcohol treatment (Fig. 3). This increase in permeability is mostly due to an increase in diffusion coefficient (See **Error! Reference source not found.**) confirming that MIL-101 has sufficiently large windows and internal cavities to allow easy access of the alcohol, in order to promote the removal of residual solvent from MIL-101 and the further passage of the gases (See **Error! Reference source not found.** and **Error! Reference source not found.** - **Error! Reference source not found.**).

The PIM-1A/MIL-101A membranes show a higher permeability compared to the PIM-1A/NanoMIL-101, PIM-1B/NH_2-MIL-101 and PIM-1B/ED-MIL-101. The effect of MIL-101 in PIM-1 is also larger than that of ZIF-8 and UiO-66 observed previously [34,35]. This is related to the very high surface area of MIL-101 and the large internal voids. The PIM-1/MIL-101-based MMMs maintain the same gas permeation order of PIM-1 itself, with CO_2 as the most permeable species. An increasing volume fraction of MIL-101A, NanoMIL-101 and MIL-101B results in a higher permeability for all gases (Fig. 3A). This is in agreement with the tendency reported by Naseri *et al.* for Matrimid©/MIL-101 [50] and by Alentiev *et al.*[29] for PIM-1/MIL-101, which with a loading of only 33% of MIL-101 increased the CO_2 permeability of the neat PIM-1 about 3 fold. On the other hand, ED-MIL-101 and NH_2-MIL-101 only moderately increased the permeability of neat PIM-1B. This trend is similar to that observed by Ma et al. [51], who reached a maximum loading of only 15 vol% NH_2-MIL-101 and remarkably found a 3 times lower permeability. A decrease of the permeability of the alcohol treated PIM-1 membranes in the presence of NH_2-MIL-101 was also observed by Isaeva *et al.*[52]. Also NH_2-modified UiO and NH_2-modified Porous Organic Polymers (POP) give only a modest increased in permeability of PIM-1, similar to those achieved with NH_2-

MIL-101 [53,54]. ED-MIL-101 does not give any improvement of the PIM-1 permeability, and over the entire composition range, the membranes with ED-MIL-101 are less permeable than those with NH_2-MIL-101, probably due to a larger steric hindrance by the longer ethylenediamine groups.
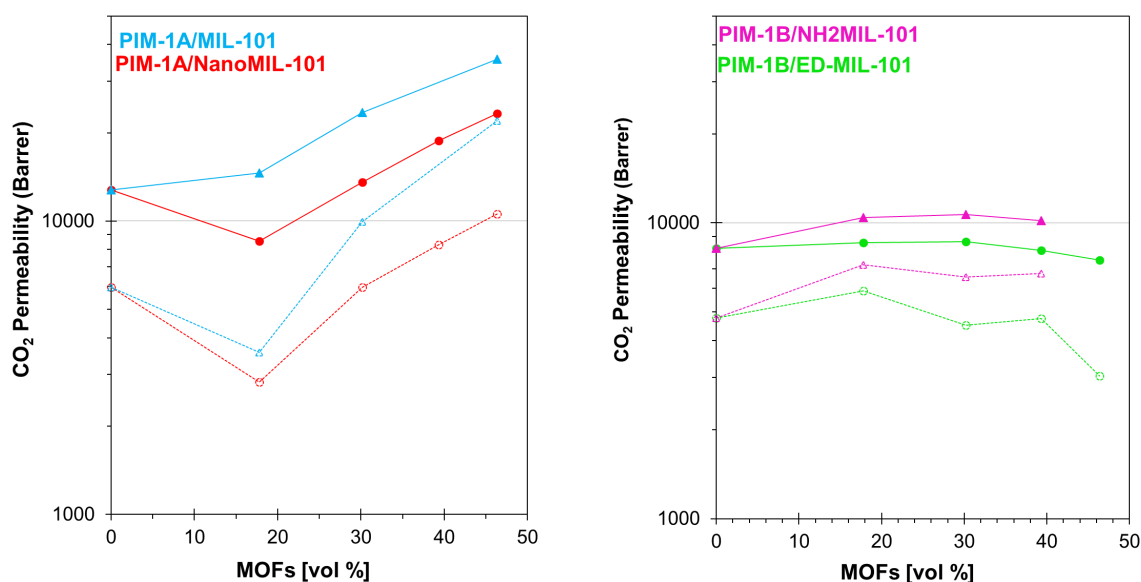

Fig. 3. (A) CO_2 permeability coefficient of PIM-1 loaded with MIL-101 (blue) and NanoMIL-101(red) and (B) PIM-1B with NH_2-MIL-101(pink) and ED-MIL-101(green). Filled symbols for "as cast" and open symbols for alcohol treated membranes.

The changes in permeability induced by the MOFs are mostly caused by an increase in the diffusion coefficient, which clearly increases with the MIL-101 concentration (**Error! Reference source not found.**), and a slight reduction of the solubility (**Error! Reference source not found. - Error! Reference source not found.**). The enhanced diffusion for NanoMIL-101, MIL-101A and MIL-101B indicates transport within the pore structure of the crystalline MOF. Both the as-cast (**Error! Reference source not found.**) and the alcohol-treated membranes (Fig. 3A) have a substantially higher permeability with MIL-101A than with the equivalent NanoMIL-101. The lower permeability of the NanoMIL-101 samples suggests the presence of a densified interface layer that hinders access to the internal voids. Instead, at higher loadings, the internal voids in the unfunctionalized MIL-101 crystals and/or inter-crystal voids start dominating the transport properties, so that the permeability tends to

increase gradually with increasing filler loading. A similar increase was previously observed for PIM-1 containing ZIF-8 [34] and purely organic cage molecules as porous fillers [55].
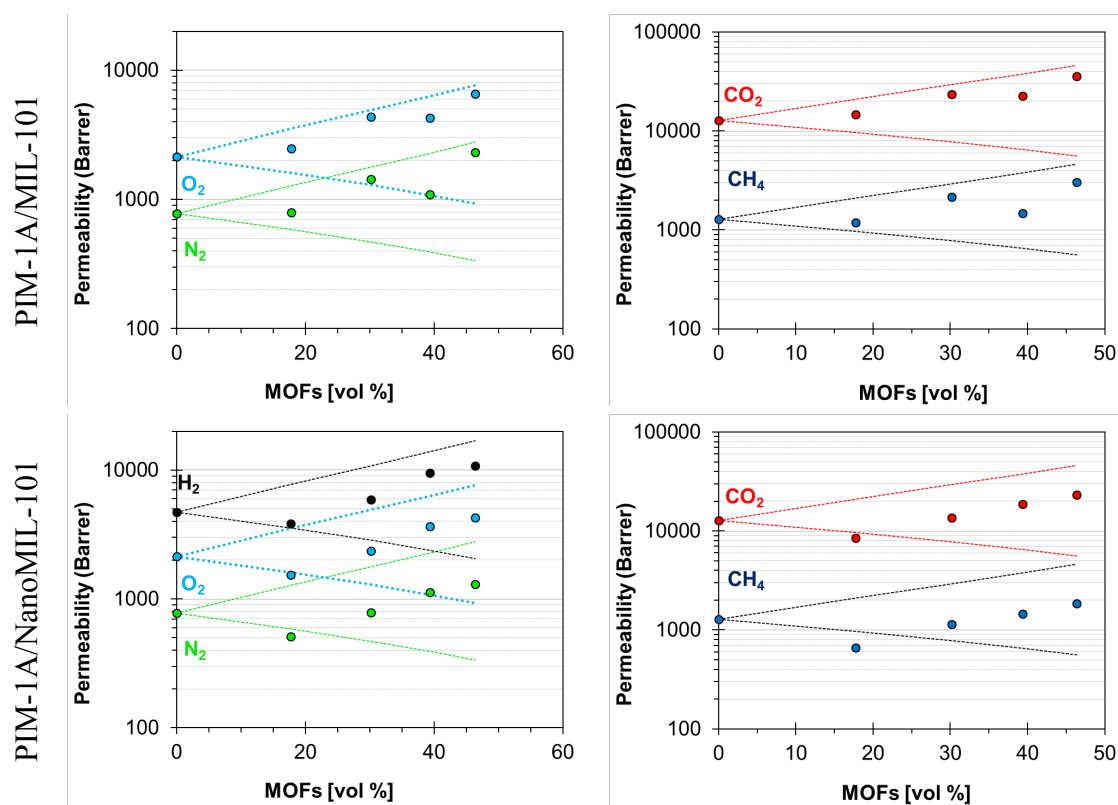

Fig. 4 H_2, O_2, N_2, CO_2, CH_4 permeabilities as function of the MOFs concentrations for PIM-1A/MIL-101 (top) and PIM-1A/NanoMIL-101 membranes (bottom). The lines represent the upper limit ($P_d=\infty$) and lower limit ($P_d=0$) of of the Maxwell equation (**Error! Reference source not found.** and **Error! Reference source not found.**), respectively. 1 Barrer = 10^{-10} cm$^3_{STP}$ cm cm^{-2} s^{-1} cmHg^{-1}

Fig. 4 shows the experimental permeabilities of CO_2 as a function of the concentration for the most significant MOFs, MIL-101 and Nano-MIL-101 MOFs in comparison with the extreme cases of the Maxwell model. The fact that the permeabilities fall within the Maxwell window, delimited by the two extreme cases of $P_d = \infty$ and $P_d = 0$, respectively indicates that the membranes are essentially defect-free. The Maxwell window is the area delimited by the dashed lines representing infinitely permeable and impermeable filler materials, as described previously [35]. Slight scatter in the data, especially of the less permeable gases, is due to the inherent difficulty to make a very good and homogeneous films from PIMs with dispersed MOFs. The systematically lower permeability at low MIL loadings, in some cases below the Maxwell limit, indicates that the filler also affects the bulk properties of the PIM, probably by occupying the largest free volume elements. At higher loadings, the volume fraction of the

MOF exceeds that of the free volume and the positive effect of the MOF dominates the overall properties.

MIL-101A based MMMs, and to a lesser extent those with Nano-MIL-101 and MIL-101B, show unprecedented permeabilities and approach the upper Maxwell limit with increasing MOF loading compared to the neat polymer. On the other hand, for ED-MIL-101 and NH_2-MIL-101, the permeabilities of most MMMs fall relatively close to the centre of the interval predicted by the Maxwell equation, which means that the permeability of these MILs is high and close to that of the polymer matrix itself.

3.2.2 Comparison of different PIM-1 batches

A consistency check of two structurally identical fillers in structurally the same polymer, but both from different batches and with different Mw (MIL-101A in PIM-1A and MIL-101B in PIM-1B), shows different absolute values, but very similar trends (Fig. 5).

This indicates that the absolute values are dictated by the PIM, and the trends are caused by the MOFs. Variability in permeability of PIMs is a well-known fact, as recently shown by Rose et al. with a cloud of data for PIM-1 from different sources in the literature [56]. We may therefore deduce that the different trends in ED-MIL-101 and NH_2-MIL-101 must indeed be attributed to the MOF itself and not to the different PIM-1 batches.
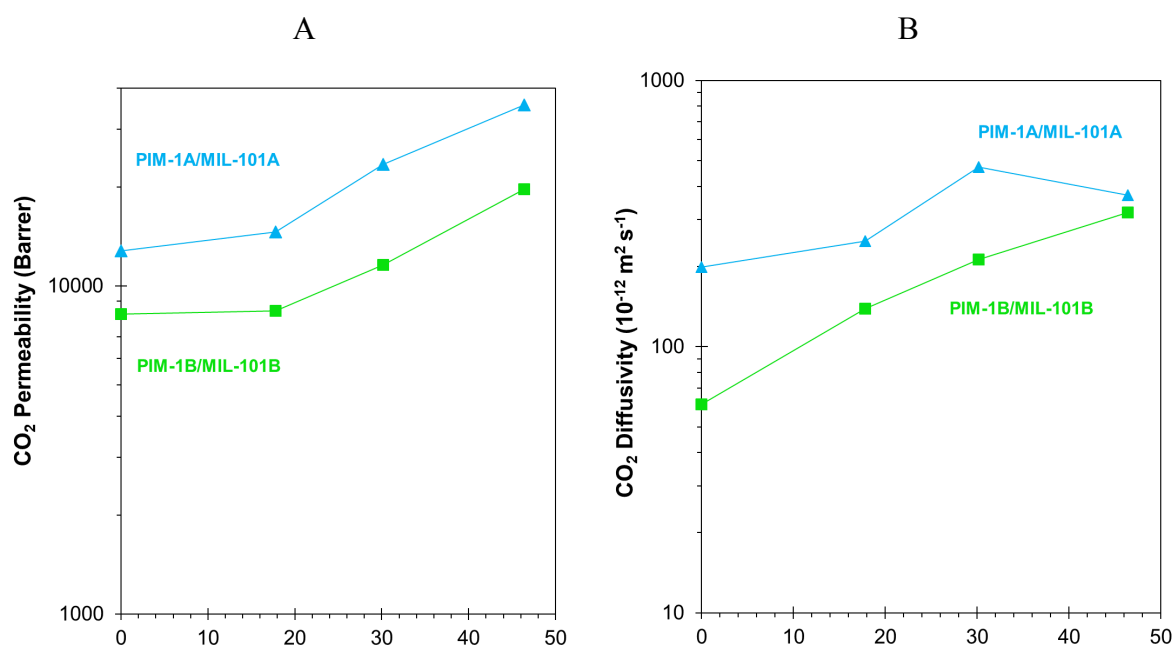

Fig. 5. Similarity of the trends of CO_2 permeabilities (A) and diffusion coefficient (B) as function of MIL-101 vol% loaded in PIM-1A and PIM-1B membranes.

3.2.3 Aging studies

Typically, amorphous glassy polymers relax over time, losing excess free volume, and hence permeability. PIMs, with their high free volume, are particularly sensitive to this. On aging, alcohol-treated PIM-1 loses much of the extra permeability gained on alcohol-treatment, both for gases [9,55,57] and for vapours [58]. In contrast, the void structure within the crystalline MOF should be stable, provided that no chemical changes or irreversible adsorption occur. Long-term aging studies were therefore performed on the most interesting set of MMMs based on MIL-101 and NanoMIL-101, because it was expected that the presence of MIL-101 might lead to similar stabilization of the permeability as with PAF fillers [20]. This stabilization was, however, not observed and the PIM-1/MIL-101 MMMs of the present work were found to lose permeability over time, coupled with a gain in selectivity. Fig. 6 shows the CO_2 permeability as a function of time for the two best performing PIM-1A/MIL-101A and PIM-1A/NanoMIL-101 MMMs after alcohol treatment.

A B

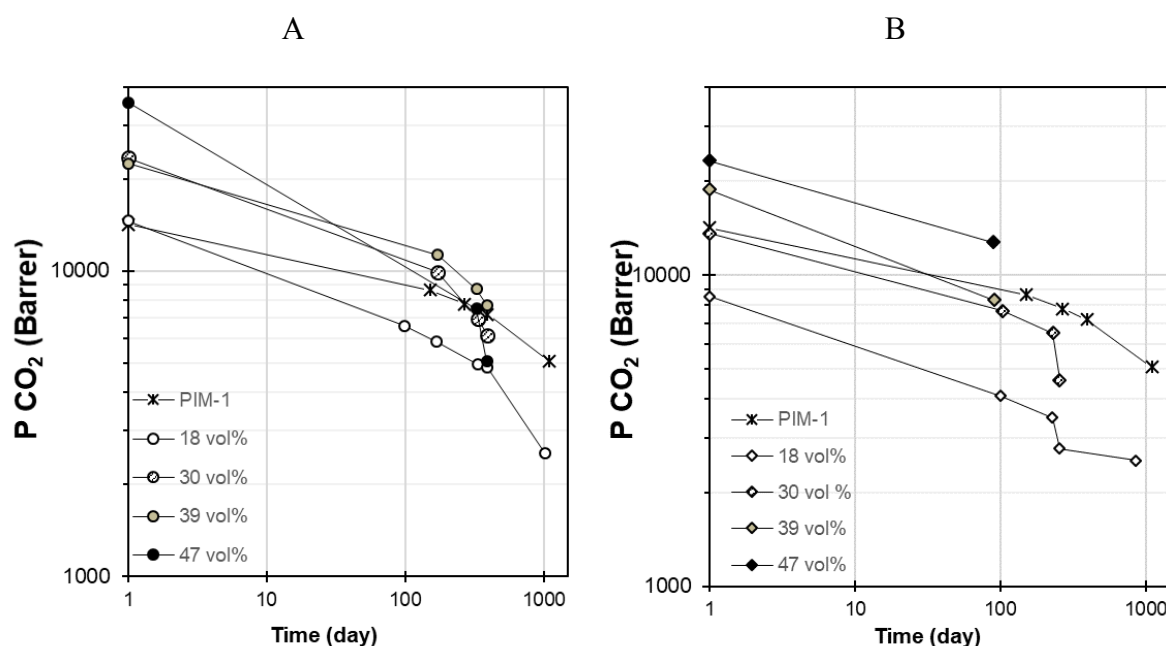**Fig. 6.** Change in CO_2 permeability over time for A) ethanol-treated PIM-1 (✶), PIM-1A/MIL-101A MMMs with 18 (O), 30 (⊘), 39 (◐) and 47vol%(●), and B) PIM-1A/NanoMIL-101 MMMs with wt. ratios 18 (◇), 30 (◈), 39 (◆) and 47 vol%(◆).

For both MIL-101 sizes, all loadings undergo a relatively similar decrease in permeability upon aging. In any case, the rate of physical aging is much slower than that in the ultra-permeable

PTMSP, which loses up to two orders of magnitude in permeability for oxygen and isobutane in 100 days [59]. Furthermore, samples with a higher initial permeability maintained this advantage over time and maintained a higher permeability than the as-cast samples. These results demonstrate that the incorporation of MIL-101 may not avoid physical aging, but it can markedly enhance the gas permeability of PIM-1 over short to medium time aging, while increasing CO_2/N_2 and CO_2/CH_4 selectivity (as it will be discussed in the next section).

3.3 *Mixed gas transport properties*

The real membrane performance for two relevant industrial separations was tested via mixed gas permeability measurements on the PIM-1A/MIL-101A sample with the highest MOF loading (47 vol%) and the highest permeability. In order to evaluate the true effect of the MOFs on the transport properties, a well-consolidated as-cast sample after 7 years of aging was tested. This sample is more representative for commercial membranes, which are normally asymmetric or thin film composite membranes, and therefore not alcohol treated. Thin films also age faster, so that the 7 years aged thick film represents a thin film with intermediate age. Measurements were performed from 1 to 6 bar(a) with two binary gas mixtures of CO_2/N_2 (15:85 vol%) and CO_2/CH_4 (35:65 vol%), simulating flue gas and biogas, respectively (Fig. 7).
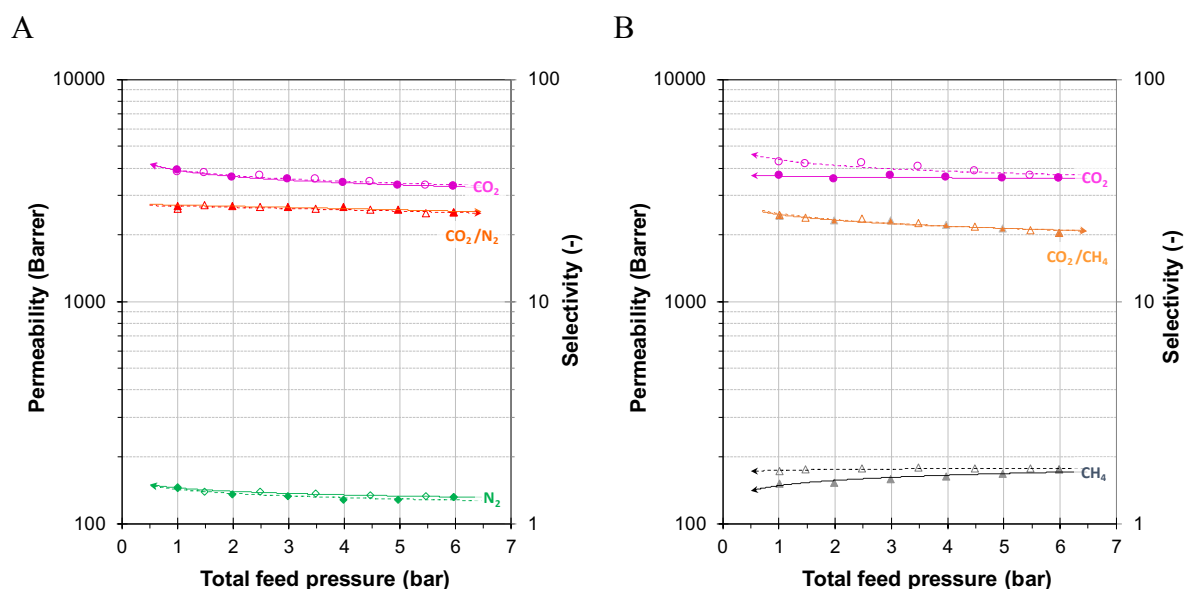

Fig. 7. A) Pressure dependence of CO_2 and N_2 permeabilities and CO_2/N_2 selectivity in binary mixture conditions for CO_2/N_2 (15:85 vol%); B) Pressure dependence of CO_2 and CH_4 permeabilities and CO_2/CH_4 selectivity using the binary CO_2/CH_4 (35:65 vol%) mixture for the PIM-1A/MIL-101A (47 vol%) membrane aged for 7 years. Closed symbols for

stepwise increase of the pressure and open symbols for the subsequent stepwise decrease of the pressure.

The synthetic flue gas mixture shows typical dual mode behaviour, with a decrease of CO_2 permeability as a function of the feed pressure. Occupation of the free volume by CO_2 causes a simultaneous and slightly smaller decrease of the N_2 permeability, and as a result, the selectivity slightly decreases as a function of pressure. For this mixture, there is no significant hysteresis between the pressure increase run and the pressure decrease run. On the contrary, anomalous behaviour is observed for the CO_2/CH_4 mixture. Competition between dual mode behaviour (with decreasing permeability as a function of pressure) and dilation by the high internal CO_2 and CH_4 concentrations, gives an almost constant permeability in the pressure increase run, followed by the typical dual mode behaviour on the return run. This clear hysteresis is also observed for methane, but in this case, the dilation facilitates the permeation of methane, which increases with increasing pressure and then remains virtually constant with decreasing pressure. As a consequence, the CO_2/CH_4 selectivity decreases with increasing pressure. For both mixtures, the mixed gas performance is better than the ideal selectivity measured in the time lag instrument (see Robeson plot, Fig. 8). This can be ascribed to competitive sorption of CO_2 over the less soluble gases N_2 and CH_4. Although the data move back towards the Robeson upper bound at higher pressure, all mixed gas permeation data lie above the upper bound, confirming the excellent performance of the PIM-1A/MIL-101A based MMM.

3.4 Performance overview

The results are summarized in the Robeson diagrams in Fig. 8. Alcohol-treated PIM-1A/MIL-101A membranes exhibit an extremely high CO_2 permeability (up to 35,600 Barrer for 47 vol% MIL-101). This is within the range of poly(1-trimethylsilyl-1-propyne) (PTMSP), one of the most permeable polymers reported in the literature so far [60–62], but at much higher selectivity, and it is similar to the recently reported triptycene-based PIM [63]. The CO_2/CH_4 and CO_2/N_2 separation performance of the MMMs surpasses the Robeson upper bound in the high permeability region for MIL-101 and NanoMIL-101. The permeabilities and ideal selectivities shift slightly upward into the righthand direction of the Robeson diagrams, suggesting that the polymer matrix still provides the main resistance to transport, while the fillers provide a preferential diffusion path. This effect is most evident with the larger MIL-

101 particles, which shows a higher permeability for all gases compared to the NanoMIL-101 (Fig. 8). The initial reduction in permeability compared to the neat PIM-1A at the lowest NanoMIL-101 loading (18 vol%) can be ascribed to the matrix densification near the interface, described by Moore and Koros as case I [64], or to the occupation of the largest free volume elements, as described in section 3.2.1.
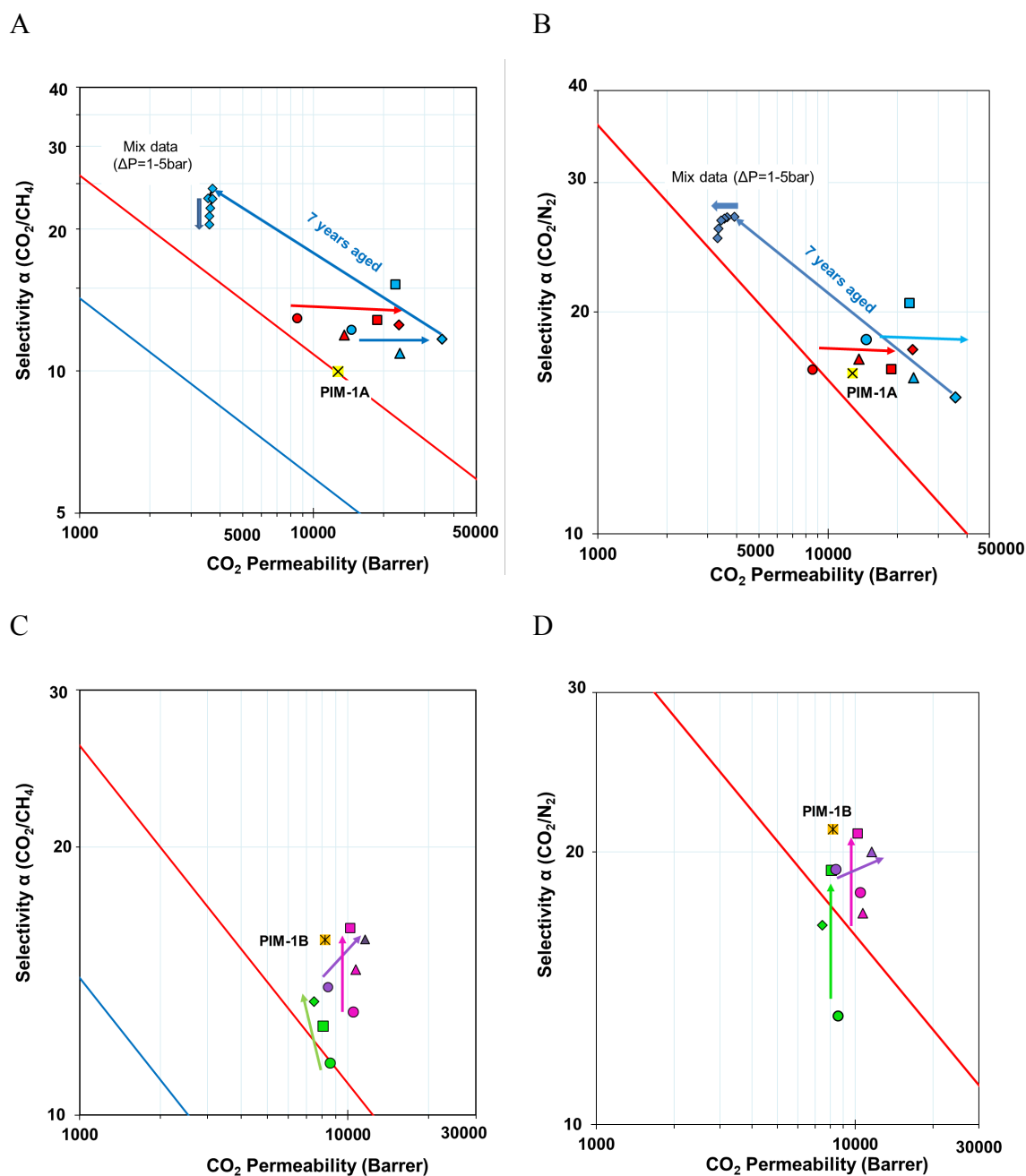

Fig. 8. Robeson's plots of CO_2/CH_4 (A,C) and CO_2/N_2 gas pairs (B,D), showing the data of ethanol treated membranes PIM-1A/MIL-101A (blue) PIM-1A/NanoMIL-101 (red), and methanol treated membranes PIM-

1B/NH$_2$-MIL-101 (pink), PIM-1B/ED-MIL-101 (green) and PIM-1B/MIL-101B (violet), at 18 vol% ◐, 30 vol% △, 39 vol% ☐ and 47 vol% ♦. Neat PIM-1A (×) PIM-1B (✖) are reported as a reference. Blue line: 1991 upper bound; red line: 2008 upper bound. [8]. The arrows serve as a guide to the eye to understand the effect of increasing MOF loading. The closely connected blue diamonds represent mixed gas data at pressures of 1-6 bar(a) for a 7 years aged PIM-1A/MIL-101A as-cast membrane with a loading of 47 vol%. 1 Barrer = 10^{-10} cm^3 [STP] cm cm^{-2} s^{-1} cmHg^{-1}.

The effect of ED-MIL-101 and NH$_2$-MIL-101 is not fundamentally different, but much smaller, and for most gases there is only a relatively small increase in permeability compared to MIL-101. For CO$_2$, this increase is contrasted by the strong affinity with the amino groups of the functionalized MIL, leading to immobilizing sorption [65,66], as was previously seen for Amine-PIM-1 [67]. Therefore, the permeability of CO$_2$ is relatively constant, and the selectivity of gas pairs involving CO$_2$ decreases. This effect if more evident for ED-MIL-101, which has more amino groups to interact with CO$_2$. Nevertheless, almost all points are still near or above the 2008 Upper Bound for important gas pairs such as CO$_2$/CH$_4$, CO$_2$/N$_2$ and close to the 2015 upper bound for O$_2$/N$_2$ and H$_2$/CH$_4$ (**Error! Reference source not found.**). The Robeson diagrams highlight especially the impressive mixed gas performance of the aged as-cast membrane sample with permeability and selectivity far exceeding the Robeson upper bound.

4   Conclusions

Mixed matrix membranes based on MIL-101, NanoMIL-101, ED-MIL-101 and NH$_2$-MIL-101 in the polymer of intrinsic microporosity PIM-1 were successfully obtained and studied for pure and mixed gas permeation. SEM analysis confirmed a good dispersion of the MOFs without evident defects at the interface. After an initial decrease in selectivity in the presence of low concentrations of NH$_2$-MIL-101 and ED-MIL-101, higher concentrations of these fillers restore the ideal gas selectivity to a value close to that of the neat PIM-1B. Nevertheless, they hardly improve the performance of the polymer itself. In contrast, pristine MIL-101 drastically increases the CO$_2$ permeability, maintaining the excellent ideal CO$_2$/N$_2$ and CO$_2$/CH$_4$ selectivity of the neat polymer. The effect of MIL-101 samples falls within the range predicted by the Maxwell model for highly permeable fillers. The extremely high CO$_2$ permeability of 35,600 Barrer is an unprecedented achievement for MMMs based on PIM-1. Studies of

permeability over time, show that MMMs with large amounts of MOFs maintain a relatively high permeability upon aging compared to neat PIM-1 over short to medium time aging. Finally, under mixed gas permeation tests, an aged as-cast PIM-1/MIL-101 MMM shows better than ideal performance, probably due to competitive sorption. The excellent combination of permeability and CO_2/N_2 selectivity (~25-27) and CO_2/CH_4 selectivity (~21-24) confirms the potential suitability of the present MMMs for use in relevant industrial gas separations such as biogas purification and CO_2 sequestration from flue gas.

Acknowledgements

References

[1]   P. Bernardo, E. Drioli, G. Golemme, Membrane gas separation: A review/state of the art, Ind. Eng. Chem. Res. 48 (2009) 4638–4663. doi:10.1021/ie8019032.

[2]   P.M. Budd, N.B. McKeown, Highly permeable polymers for gas separation membranes, Polym. Chem. 1 (2010) 63–68. doi:10.1039/b9py00319c.

[3]   N.B. McKeown, P.M. Budd, K.J. Msayib, B.S. Ghanem, H.J. Kingston, C.E. Tattershall, et al., Polymers of intrinsic microporosity (PIMs): Bridging the void between microporous and polymeric materials, Chem. - A Eur. J. 11 (2005) 2610–2620. doi:10.1002/chem.200400860.

[4]   M. Heuchel, D. Fritsch, P.M. Budd, N.B. McKeown, D. Hofmann, Atomistic packing model and free volume distribution of a polymer with intrinsic microporosity (PIM-1), J. Memb. Sci. 318 (2008) 84–99. doi:10.1016/j.memsci.2008.02.038.

[5]   P.M. Budd, E.S. Elabas, B.S. Ghanem, S. Makhseed, N.B. McKeown, K.J. Msayib, et al., Solution-Processed, Organophilic Membrane Derived from a Polymer of Intrinsic Microporosity, Adv. Mater. (2004). doi:10.1002/adma.200306053.

[6]   P.M. Budd, K.J. Msayib, C.E. Tattershall, B.S. Ghanem, K.J. Reynolds, N.B. Mckeown, et al., Gas separation membranes from polymers of intrinsic microporosity, J. Memb. Sci. 251 (2005) 263–269. doi:10.1016/j.memsci.2005.01.009.

[7]   P.M. Budd, N.B. McKeown, B.S. Ghanem, K.J. Msayib, D. Fritsch, L. Starannikova, et al., Gas permeation parameters and other physicochemical properties of a polymer of intrinsic microporosity: Polybenzodioxane PIM-1, J. Memb. Sci. 325 (2008) 851–860. doi:10.1016/j.memsci.2008.09.010.

[8]   L.M. Robeson, The upper bound revisited, J. Memb. Sci. 320 (2008) 390–400. doi:10.1016/j.memsci.2008.04.030.

[9]   P. Bernardo, F. Bazzarelli, F. Tasselli, G. Clarizia, C.R. Mason, L. Maynard-Atem, et al., Effect of physical aging on the gas transport and sorption in PIM-1 membranes, Polymer (Guildf). (2016). doi:10.1016/j.polymer.2016.10.040.

[10]   Y. Huang, D.R. Paul, Physical aging of thin glassy polymer films monitored by gas permeability, Polymer (Guildf). 45 (2004) 8377–8393. doi:10.1016/j.polymer.2004.10.019.

[11]   W. S. Harms, K. Rätzke, F. Faupel, N. Chaukura, P.M. Budd, Aging and Free Volume in a Polymer of Intrinsic Microporosity (PIM-1) Aging and Free Volume in a Polymer of Intrinsic Microporosity (PIM-1), J. Adhes. 88 (2012) 37–41. doi:10.1080/00218464.2012.682902.

[12]   H. Li, K. Wang, Y. Sun, C.T. Lollar, J. Li, H.-C. Zhou, Recent advances in gas storage and separation using metal–organic frameworks, Mater. Today. 21 (2018) 108–121. doi:10.1016/J.MATTOD.2017.07.006.

[13]   R.D. Noble, Perspectives on mixed matrix membranes, J. Memb. Sci. 378 (2011) 393–397. doi:10.1016/j.memsci.2011.05.031.

[14]   J. Ahn, W.-J. Chung, I. Pinnau, J. Song, N. Du, G.P. Robertson, et al., Gas transport behavior of mixed-matrix membranes composed of silica nanoparticles in a polymer of intrinsic microporosity (PIM-1), J. Memb. Sci. 346 (2010) 280–287. doi:10.1016/j.memsci.2009.09.047.

[15]   G. Dong, H. Li, V. Chen, Challenges and opportunities for mixed-matrix membranes for gas separation, J. Mater. Chem. A. 1 (2013) 4610–4630. doi:10.1039/C3TA00927K.

[16]   M.A. Rodrigues, J. de S. Ribeiro, E. de S. Costa, J.L. de Miranda, H.C. Ferraz, Nanostructured membranes containing UiO-66 (Zr) and MIL-101 (Cr) for O2/N2and CO2/N2separation, Sep. Purif. Technol. (2018). doi:10.1016/j.seppur.2017.10.024.

[17] Y. Cheng, Z. Wang, D. Zhao, Mixed Matrix Membranes for Natural Gas Upgrading: Current Status and Opportunities, Ind. Eng. Chem. Res. 57 (2018) 4139–4169. doi:10.1021/acs.iecr.7b04796.

[18] M.A.A. Aroon, A.F.F. Ismail, T. Matsuura, M.M.M. Montazer-Rahmati, Performance studies of mixed matrix membranes for gas separation: A review, Sep. Purif. Technol. 75 (2010) 229–242. doi:10.1016/j.seppur.2010.08.023.

[19] Y. Yampolskii, Polymeric Gas Separation Membranes, 45 (2012) 3298–3311.

[20] C.H. Lau, P.T. Nguyen, M.R. Hill, A.W. Thornton, K. Konstas, C.M. Doherty, et al., Ending aging in super glassy polymer membranes, Angew. Chemie - Int. Ed. 53 (2014) 5322–5326. doi:10.1002/anie.201402234.

[21] L. Olivieri, S. Meneguzzo, S. Ligi, A. Saccani, L. Giorgini, A. Orsini, et al., Reducing ageing of thin PTMSP films by incorporating graphene and graphene oxide: effect of thickness, gas type and temperature, J. Memb. Sci. (2018). doi:10.1016/J.MEMSCI.2018.03.056.

[22] S. Rochat, K. Polak-Kraśna, M. Tian, L.T. Holyfield, T.J. Mays, C.R. Bowen, et al., Hydrogen storage in polymer-based processable microporous composites, J. Mater. Chem. A. 5 (2017) 18752–18761. doi:10.1039/c7ta05232d.

[23] C.R. Mason, M.G. Buonomenna, G. Golemme, P.M. Budd, F. Galiano, A. Figoli, et al., New organophilic mixed matrix membranes derived from a polymer of intrinsic microporosity and silicalite-1, Polym. (United Kingdom). 54 (2013) 2222–2230. doi:10.1016/j.polymer.2013.02.032.

[24] M.M. Khan, V. Filiz, G. Bengtson, M.M. Rahman, S. Shishatskiy, V. Abetz, Functionalized Carbon Nanotube Mixed Matrix Membranes of Polymers of Intrinsic Microporosity (PIMs) for Gas Separation, Procedia Eng. 44 (2012) 1899–1901. doi:http://dx.doi.org/10.1016/j.proeng.2012.08.997.

[25] K. Althumayri, W.J. Harrison, Y. Shin, J.M. Gardiner, C. Casiraghi, P.M. Budd, et al., The influence of few-layer graphene on the gas permeability of the high-free-volume polymer PIM-1, Philos. Trans. R. Soc. A Math. Phys. Eng. Sci. 374 (2016) 20150031. doi:10.1098/rsta.2015.0031.

[26] M.M. Khan, S. Shishatskiy, V. Filiz, Mixed matrix membranes of boron icosahedron and polymers of intrinsic microporosity (PIM-1) for gas separation, Membranes (Basel). 8 (2018) 1–18. doi:10.3390/membranes8010001.

[27] O.M. Yaghi, H. Li, C. Davis, D. Richardson, T.L. Groy, Synthetic Strategies , Structure

Patterns , and Emerging Properties in the Chemistry of Modular Porous Solids †
Decorated Diamond Nets : Porous Metal, 31 (1998) 474–484.

[28] O.K. Farha, J.T. Hupp, Activation of Metal - Organic Framework Materials, Chem. Res.
43 (2010) 1166–1175.

[29]   a. Y. Alentiev, G.N. Bondarenko, Y. V. Kostina, V.P. Shantarovich, S.N. Klyamkin,
V.P. Fedin, et al., PIM-1/MIL-101 hybrid composite membrane material: Transport
properties and free volume, Pet. Chem. 54 (2014) 477–481.
doi:10.1134/S0965544114070020.

[30] R. Castro-Muñoz, V. Fíla, C.T. Dung, Mixed Matrix Membranes Based on PIMs for
Gas Permeation: Principles, Synthesis, and Current Status, Chem. Eng. Commun. 204
(2017) 295–309. doi:10.1080/00986445.2016.1273832.

[31] H.B.T. Jeazet, T. Koschine, C. Staudt, K. Raetzke, C. Janiak, Correlation of Gas
Permeability in a Metal-Organic Framework MIL-101(Cr)–Polysulfone Mixed-Matrix
Membrane with Free Volume Measurements by Positron Annihilation Lifetime
Spectroscopy (PALS), 3 (2013) 331–353. doi:10.3390/membranes3040331.

[32] H.B. Tanh Jeazet, C. Staudt, C. Janiak, Metal-organic frameworks in mixed-matrix
membranes for gas separation, Dalt. Trans. 41 (2012) 14003–14027.
doi:10.1039/c2dt31550e.

[33] A. Fuoco, M. Khdhayyer, M. Attfield, E. Esposito, J. Jansen, P. Budd, Synthesis and
Transport Properties of Novel MOF/PIM-1/MOF Sandwich Membranes for Gas
Separation, Membranes (Basel). 7 (2017) 1–17. doi:10.3390/membranes7010007.

[34] A.F. Bushell, M.P. Attfield, C.R. Mason, P.M. Budd, Y. Yampolskii, L. Starannikova,
et al., Gas permeation parameters of mixed matrix membranes based on the polymer of
intrinsic microporosity PIM-1 and the zeolitic imidazolate framework ZIF-8, J. Memb.
Sci. 427 (2013) 48–62. doi:10.1016/j.memsci.2012.09.035.

[35] M.R. Khdhayyer, E. Esposito, A. Fuoco, M. Monteleone, L. Giorno, J.C. Jansen, et al.,
Mixed matrix membranes based on UiO-66 MOFs in the polymer of intrinsic
microporosity PIM-1, Sep. Purif. Technol. 173 (2017) 304–313.
doi:10.1016/J.SEPPUR.2016.09.036.

[36] G. Férey, C. Mellot-Draznieks, C. Serre, F. Millange, J. Dutour, S. Surblé, et al., A
chromium terephthalate-based solid with unusually large pore volumes and surface
area., Science. 309 (2005) 2040–2042. doi:10.1126/science.1116275.

[37] J.P. Jung, M.J. Kim, Y.S. Bae, J.H. Kim, Facile preparation of Cu(I) impregnated MIL-

101(Cr) and its use in a mixed matrix membrane for olefin/paraffin separation, J. Appl. Polym. Sci. 135 (2018) 1–8. doi:10.1002/app.46545.

[38] W. Zhang, Y. Ying, J. Ma, X. Guo, H. Huang, D. Liu, et al., Mixed matrix membranes incorporated with polydopamine-coated metal-organic framework for dehydration of ethylene glycol by pervaporation, J. Memb. Sci. 527 (2017) 8–17. doi:10.1016/J.MEMSCI.2017.01.001.

[39] H.B. Tanh Jeazet, S. Sorribas, J.M. Román-Marín, B. Zornoza, C. Téllez, J. Coronas, et al., Increased Selectivity in CO2/CH4Separation with Mixed-Matrix Membranes of Polysulfone and Mixed-MOFs MIL-101(Cr) and ZIF-8, Eur. J. Inorg. Chem. 2016 (2016) 4363–4367. doi:10.1002/ejic.201600190.

[40] G. Férey, C. Mellot-Draznieks, C. Serre, F. Millange, J. Dutour, S. Surblé, et al., A Chromium Terephtalate-Based Solid with Unusually Large Pore Volumes and Surface Area, Science (80-.). 309 (2005) 2040. doi:10.1126/science.1116275.

[41] N. Du, G.P. Robertson, J. Song, I. Pinnau, S. Thomas, M.D. Guiver, Polymers of intrinsic microporosity containing trifluoromethyl and phenylsulfone groups as materials for membrane gas separation, Macromolecules. 41 (2008) 9656–9662. doi:10.1021/ma801858d.

[42] P.L. Llewellyn, S. Bourrelly, C. Serre, A. Vimont, M. Daturi, L. Hamon, et al., High uptakes of CO2 and CH4 in mesoporous metal-organic frameworks MIL-100 and MIL-101, Langmuir. 24 (2008) 7245–7250. doi:10.1021/la800227x.

[43] L. Bromberg, Y. Diao, H. Wu, S.A. Speakman, T.A. Hatton, Chromium(III) terephthalate metal organic framework (MIL-101): Hf-free synthesis, structure, polyoxometalate composites, and catalytic properties, Chem. Mater. 24 (2012) 1664–1675. doi:10.1021/cm2034382.

[44] D. Jiang, A.D. Burrows, K.J. Edler, Size-controlled synthesis of MIL-101(Cr) nanoparticles with enhanced selectivity for CO2 over N2, CrystEngComm. (2011). doi:10.1039/c1ce06274c.

[45] Y.K. Hwang, D.-Y. Hong, J.-S. Chang, S.H. Jhung, Y.-K. Seo, J. Kim, et al., Amine grafting on coordinatively unsaturated metal centers of MOFs: Consequences for catalysis and metal encapsulation, Angew. Chemie - Int. Ed. 47 (2008) 4144–4148. doi:10.1002/anie.200705998.

[46] Y. Lin, C. Kong, L. Chen, Direct synthesis of amine-functionalized MIL-101(Cr) nanoparticles and application for CO<inf>2</inf> capture, RSC Adv. 2

(2012) 6417–6419. doi:10.1039/c2ra20641b.

[47]   J.C. Jansen, K. Friess, E. Drioli, Organic vapour transport in glassy perfluoropolymer membranes: A simple semi-quantitative approach to analyze clustering phenomena by time lag measurements, J. Memb. Sci. 367 (2011) 141–151. doi:10.1016/j.memsci.2010.10.063.

[48]   J. Crank, The mathematics of diffusion, 2nd ed., Clarendon Press, Oxford, 1975.

[49]   S.C. Fraga, M. Monteleone, M. Lanč, E. Esposito, A. Fuoco, L. Giorno, et al., A novel time lag method for the analysis of mixed gas diffusion in polymeric membranes by on-line mass spectrometry: Method development and validation, J. Memb. Sci. 561 (2018) 39–58. doi:10.1016/J.MEMSCI.2018.04.029.

[50]   M. Naseri, S.F. Mousavi, T. Mohammadi, O. Bakhtiari, Synthesis and gas transport performance of MIL-101/Matrimid mixed matrix membranes, J. Ind. Eng. Chem. 29 (2015) 249–256. doi:10.1016/j.jiec.2015.04.007.

[51]   J. Ma, Y. Ying, X. Guo, H. Huang, D. Liu, C. Zhong, Fabrication of mixed-matrix membrane containing metal-organic framework composite with task-specific ionic liquid for efficient CO2 separation, J. Mater. Chem. A. 4 (2016) 7281–7288. doi:10.1039/c6ta02611g.

[52]   L.M.K. V. I. Isaeva, A. L. Tarasov, a L. E. Starannikova, Yu. P. Yampol´skii, A. Yu. Alent´ev, Microwave assisted synthesis of mesoporous metal organic framework NH2-MIL-101(Al), Russ. Chem. Bull. Int. Ed. 64 (2015) 2791–2795.

[53]   Z. Wang, H. Ren, S. Zhang, F. Zhang, J. Jin, Polymers of intrinsic microporosity/metal–organic framework hybrid membranes with improved interfacial interaction for high-performance CO2 separation, J. Mater. Chem. A. 5 (2017) 10968–10977. doi:10.1039/C7TA01773A.

[54]   C. Wang, F. Guo, H. Li, J. Xu, J. Hu, H. Liu, Porous organic polymer as fillers for fabrication of defect-free PIM-1 based mixed matrix membranes with facilitating CO2-transfer chain, J. Memb. Sci. 564 (2018) 115–122. doi:10.1016/J.MEMSCI.2018.07.018.

[55]   A.F. Bushell, P.M. Budd, M.P. Attfield, J.T.A. Jones, T. Hasell, A.I. Cooper, et al., Nanoporous Organic Polymer/Cage Composite Membranes, Angew. Chemie Int. Ed. 52 (2013) 1253–1256. doi:10.1002/anie.201206339.

[56]   I. Rose, C.G. Bezzu, M. Carta, B. Comesanã-Gándara, E. Lasseuguette, M.C. Ferrari, et al., Polymer ultrapermeability from the inefficient packing of 2D chains, Nat. Mater. 16

(2017) 932–937. doi:10.1038/nmat4939.

[57] R.R. Tiwari, J. Jin, B.D. Freeman, D.R. Paul, Physical aging, CO2 sorption and plasticization in thin films of polymer with intrinsic microporosity (PIM-1), J. Memb. Sci. 537 (2017) 362–371. doi:10.1016/j.memsci.2017.04.069.

[58] K. Pilnáček, O. Vopička, M. Lanč, M. Dendisová, M. Zgažar, P.M. Budd, et al., Aging of polymers of intrinsic microporosity tracked by methanol vapour permeation, J. Memb. Sci. 520 (2016) 895–906. doi:http://dx.doi.org/10.1016/j.memsci.2016.08.054.

[59] H. Shimomura, K. Nakanishi, H. Odani, M. Kurata, T. Masuda, T. Higashimura, Permeation of Gases in Poly[1-(trimethylsiiyl)-1-propyne], KOBUNSHI RONBUNSHU. 43 (1986) 747–753. doi:10.1295/koron.43.747.

[60] T. Masuda, Y. Iguchi, B.Z. Tang, T. Higashimura, Diffusion and solution of gases in substituted polyacetylene membranes, Polymer (Guildf). 29 (1988) 2041–2049. doi:10.1016/0032-3861(88)90178-4.

[61] I. Pinnau, C. G. Casillas, A. Morisato, B. D. Freeman, Hydrocarbon / Hydrogen Mixed Gas Permeation, Polym. Sci. Part B Polym. Phys. 34 (1996) 2613–2621.

[62] Y. Hu, M. Shiotsuki, F. Sanda, B.D. Freeman, T. Masuda, Synthesis and Properties of Indan-Based Polyacetylenes That Feature the Highest Gas Permeability among All the Existing Polymers, Macromolecules. 41 (2008) 8525–8532.

[63] I. Rose, M. Carta, R. Malpass-Evans, M.-C. Ferrari, P. Bernardo, G. Clarizia, et al., Highly Permeable Benzotriptycene-Based Polymer of Intrinsic Microporosity, ACS Macro Lett. 4 (2015) 912–915. doi:10.1021/acsmacrolett.5b00439.

[64] T.T. Moore, W.J. Koros, Non-ideal effects in organic–inorganic materials for gas separation membranes, J. Mol. Struct. 739 (2005) 87–98. doi:10.1016/j.molstruc.2004.05.043.

[65] D.R. Paul, Effect of immobilizing adsorption on the diffusion time lag, J. Polym. Sci. Part A-2 Polym. Phys. 7 (1969) 1811–1818. doi:10.1002/pol.1969.160071015.

[66] Z. Grzywna, J. Podkowka, Effect of immobilizing adsorption on mass transport through polymer films, J. Memb. Sci. 8 (1981) 23–31. doi:10.1016/S0376-7388(00)82136-5.

[67] C.R. Mason, L. Maynard-Atem, K.W.J. Heard, B. Satilmis, P.M. Budd, K. Friess, et al., Enhancement of CO2 Affinity in a Polymer of Intrinsic Microporosity by Amine Modification., Macromolecules. 47 (2014) 1021–1029. doi:10.1021/ma401869p.

[68] D.H. Everett, Manual of symbols and terminology for physicochemical quantities and units, Pure Appl. Chemestry. 31 (1971) 577–638.

[69] B. Shimekit, H. Mukhtar, T. Murugesan, Prediction of the relative permeability of gases in mixed matrix membranes, J. Memb. Sci. 373 (2011) 152–159. doi:10.1016/j.memsci.2011.02.038.

[70] J.C. Maxwell, A Treatise on Electricity and Magnetism Volume 1, Cambridge University Press, 2010.